

Faulted surface layers in dysprosium silicide nanowires

Zhian He,¹ David J. Smith,^{2,3} and P. A. Bennett³

¹*Science and Engineering of Materials, Arizona State University, Tempe, Arizona 85287, USA*

²*Center for Solid State Science, Arizona State University, Tempe, Arizona 85287, USA*

³*Department of Physics and Astronomy, Arizona State University, Tempe, Arizona 85287, USA*

(Received 20 April 2004; revised manuscript received 18 August 2004; published 10 December 2004)

The crystallography and microstructure of epitaxial dysprosium silicide nanowires on Si(001) have been studied using high-resolution transmission electron microscopy. Islands grown at 750 °C have a compact three-dimensional shape and are identified as hexagonal DySi₂. Islands grown at 650 °C have an elongated nanowire (NW) shape. They contain one or two layers of hexagonal silicide at the buried interface and two to three surface layers with faulted stacking similar to tetragonal DySi₂. The faulted layers are believed to provide stress relief during growth of the coherently strained NW islands.

DOI: 10.1103/PhysRevB.70.241402

PACS number(s): 68.35.Fx, 68.37.Lp, 68.55.Jk

It has recently been found that several rare-earth (RE) metals can form self-assembled epitaxial nanowires (NWs) on Si(001) with typical dimensions of 1 nm high \times 10 nm wide \times 1 μ m long.^{1–6} Self-assembled silicide NW formation has also been reported in other silicide systems including Pt/Si(001),⁷ Ti/Si(111),^{8,9} Dy/Si(110),¹⁰ and Gd/Si(111).¹¹ It is suspected that these NWs are metallic, although resistivity has not yet been directly measured for any such structures. Epitaxial silicide NWs may find application as low resistance interconnects or as nanoelectrodes for attaching small electrically active structures, possibly molecules. Silicides have favorable attributes in this regard, including low resistivity, metallurgical stability, atomically flat surface and interface, and electrical isolation from the substrate, via the Schottky barrier.^{12–15}

The size and shape of the RE/Si(001) NWs and their interaction with substrate steps has been well documented, yet the fundamental mechanism that generates the long thin NW shape is not fully understood. It is suggested that the NW shape results from anisotropic lattice mismatch between the silicide and the substrate.⁵ Thus, a large ($\sim 7\%$) mismatch in one direction limits the width of the NW, while a small ($< 1\%$) mismatch in the orthogonal direction allows essentially unlimited length of the NW. In practice, the NW length is only limited by collision with other NWs at right angles, and can exceed 1 μ m. This model assumes a hexagonal silicide lattice with its *c* axis oriented along the width of the NW. Scanning tunneling microscopy (STM) measurements of the surface unit cell and the step height are consistent with this assumption.³ However, there are two other bulk phases in these silicides, with tetragonal and orthorhombic unit cells, which are related to the hexagonal structure by a shearing of layers parallel to Si(001) and small adjustments of the (relabelled) lattice parameters, as shown in Table I and Fig. 1.¹⁶ These silicide structures are not distinguishable using STM, nor with plan-view TEM, since the surface unit cells and projected structures have the same symmetry. The unit cells will also have the same dimensions, if the island is fully strained to match the substrate. These structures also cannot be distinguished on the basis of STM-measured step

height, given the uncertain influence of electronic structure effects.³ Thus, the crystal structure of RE silicide NWs on Si(001) remains unknown.

The morphology of RE silicide islands grown on Si(001) by reactive deposition depends on temperature. Generally, NWs form at 600 °C while more compact three-dimensional (3D) islands form at higher temperatures or with extensive annealing at 650 °C.³ It has been suggested that the compact 3D islands are tetragonal silicide.³ This interpretation, however, is subject to the uncertainties noted above.

The issue of crystal structure can only be resolved using a technique that is sensitive to buried layers. In this paper, we present cross-sectional high-resolution transmission electron microscopy (HRTEM) measurements of Dy/Si(001) islands for both island types. We find that compact 3D islands grown at 750 °C are fully relaxed hexagonal DySi₂. The NW islands grown at 650 °C contain one or two layers of hexagonal silicide at the buried interface and two to three surface layers with a faulted stacking similar to tetragonal DySi₂. The faulted surface layers are believed to provide stress relief during growth of the NW islands.

Samples of *n*-type Si(001) with nominal miscut of $\pm 0.5^\circ$ and resistivity 1 Ω cm were prepared by flashing for 30 s at 1250 °C in ultrahigh vacuum (UHV). Dysprosium was deposited by sublimation from a high-purity foil. Coverage was determined *in situ* using a crystal oscillator as well as *ex situ* using atomic force microscopy (AFM) and Rutherford

TABLE I. Bulk lattice parameters for various DySi₂ structures. *h* is the layer spacing in the surface normal direction, using $\sqrt{3}/2 a$ for hexagonal and *c*/4 for tetragonal and orthorhombic.

Structure	Prototype	Lattice constant (Å)			
		<i>a</i>	<i>b</i>	<i>c</i>	<i>h</i> (Å)
Hexagonal	AlB ₂	3.83	3.83	4.12	3.32
Tetragonal	ThSi ₂	4.03	4.03	13.38	3.34
Orthorhombic	GdSi ₂	4.04	3.95	13.34	3.33

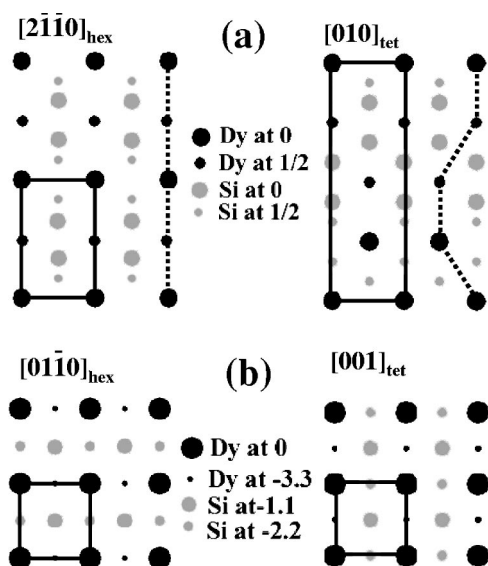


FIG. 1. Projected lattice structures for hexagonal and tetragonal dysprosium silicide shown (a) along $\text{DySi}_2\text{-hex}[2\bar{1}10] \parallel \text{DySi}_2\text{-tet}[010] \parallel \text{Si}[1\bar{1}0]$ (cross-sectional view, corresponding to HREM images), and (b) along $\text{Si}[001]$ (plan view, corresponding to the substrate normal). A single rectangular unit cell is outlined for each lattice (solid line) and dotted lines trace the straight vs staggered alignment of hexagonal vs tetragonal stacking, respectively.

backscattering on selected samples. One monolayer (ML) coverage is defined as 6.78×10^{14} Dy atoms/cm². Silicide islands were grown by reactive deposition, with approximate doses of 1 ML during 2 min while holding the substrate temperature at 650 or 750 °C. They were quenched immediately after deposition to prevent alteration of the island structure by annealing. Samples of both island type were capped with 20 nm Ti at room temperature before removal from UHV to prevent oxidation. NWs were not visible on uncoated samples. While it is possible that the cap layer destroys some features of the surface, it is not likely to induce a new ordered structure and certainly not a different one on the two types of island. AFM was done *ex situ* on a Digital Instruments MultiMode III operated in contact mode. HRTEM observations were made with a JEOL 4000EX electron microscope operated at 400 keV. Samples were prepared with standard methods of mechanical polishing, dimpling, and ion-beam milling to perforation. Images were taken at “optimum defocus” so that atomic columns appear dark, but the contrast has been inverted in the printed figures to improve visibility.

Island morphology was found to depend sensitively on growth temperature, as shown in Fig. 2. Islands grown at 650 °C had highly elongated NW shapes with typical dimensions 2 nm high, 15 nm wide, and 500 nm long. These islands are somewhat larger than those grown at 600 °C, and measured with STM, but they retain the large aspect ratio characteristic of NWs.³ Islands grown at 750 °C had compact 3D shapes with typical dimensions 5 nm high, 50 nm wide, and 200 nm long. In both cases, the long axes of the islands were oriented along the two equivalent $\text{Si}\langle 220 \rangle$ directions with equal probability. The use of these two growth tempera-

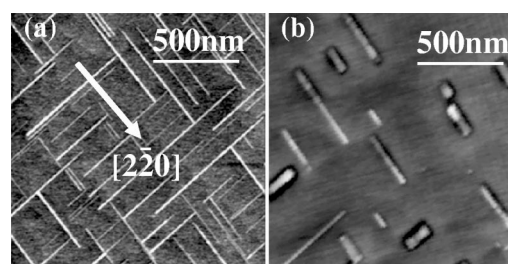


FIG. 2. AFM images of dysprosium silicide islands grown by depositing ~ 1 ML Dy on $\text{Si}(001)$ at two different temperatures: (a) 650 and (b) 750 °C. The scale and orientation are matched for the two images.

tures allowed a clear separation of the two island types. In contrast, growth at intermediate temperatures or with various annealing conditions produced coexisting island types.

Figure 3 is a HRTEM micrograph for a compact 3D island grown at 750 °C, viewed along the long axis of the island. This particular island is ~ 40 nm wide and ~ 4 nm thick. Using the adjacent Si lattice image as an internal calibration, the measured plane spacing is 4.08 ± 0.05 Å in the horizontal direction and 3.30 ± 0.05 Å in the vertical direction. The distinct layer-stacking sequence allows positive identification of this structure as hexagonal DySi_2 with orientation $\text{DySi}_2(01\bar{1}0) \parallel \text{Si}(001)$ and $\text{DySi}_2[2\bar{1}10] \parallel \text{Si}[1\bar{1}0]$. This stacking continues up to the surface layers. The measured lattice spacing parallel with the surface agrees closely with bulk hexagonal DySi_2 , suggesting that the island is essentially strain free. The stoichiometry of hexagonal dysprosium silicide in bulk equilibrium is a vacancy structure with average stoichiometry $\text{DySi}_{1.6}$. We cannot determine stoichiometry in this experiment, so we will refer to this structure as DySi_2 for simplicity. The buried interface for this island is not flat, but extends into the substrate with down steps on one side and up steps on the other. Most of these steps are one bilayer high, and have a lateral spacing ~ 4 nm.

Figure 4 shows HRTEM micrographs for two NW islands grown at 650 °C, viewed along the long axes of the islands. The NW in panel (a) has dimensions 6 nm wide and six layers thick. This NW clearly shows hexagonal stacking of the first two layers but tetragonal stacking of the top four layers, with orientation: $\text{DySi}_2(001) \parallel \text{Si}(001)$ and

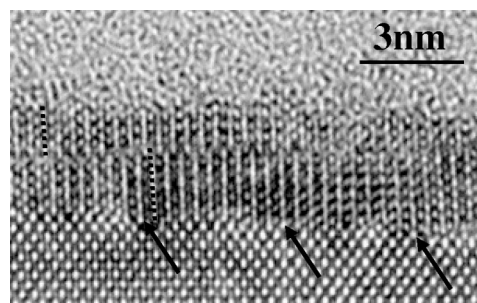


FIG. 3. High-resolution electron micrograph along $\text{Si}[1\bar{1}0]$ showing part of a compact 3D island grown at 750 °C. Arrows indicate single substrate steps at the interface. This island is identified as hexagonal DySi_2 .

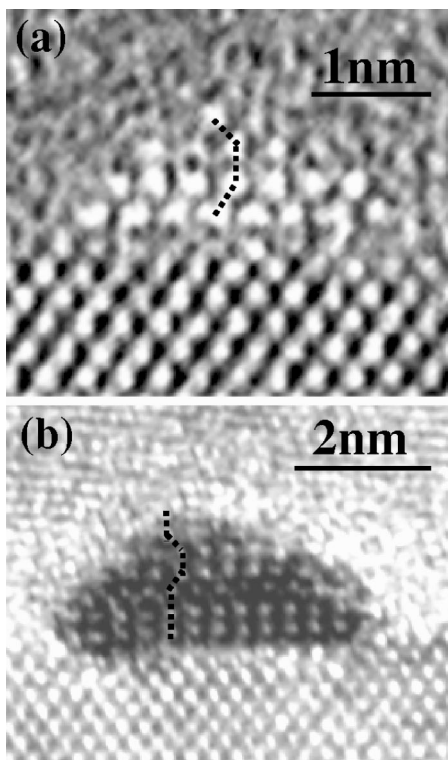


FIG. 4. High-resolution electron micrograph along $\text{Si}[\bar{1}10]$ showing two NWs of different width. Both NWs show faulted surface layers, similar to tetragonal DySi_2 , as indicated by the staggered alignment of Dy atom columns (dotted lines).

$\text{DySi}_2[010] \parallel \text{Si}[\bar{1}10]$ (long axis). The top layers are narrower and/or incomplete. The NW in panel (b) has dimensions 3 nm wide and three to four layers thick. The surface layers again follow the tetragonal lattice, while the interface layer is not resolved. Images from \sim ten different NWs showed a similar staggered alignment of surface layers on top of one or two hexagonal layers at the interface. The inverted sequence (hexagonal on top of tetragonal) was never observed.

One issue in the present study is the observation that the hexagonal phase appears at higher growth temperature than the tetragonal phase. This seems to contradict the behavior for extended thin films in the closely related $\text{Er}/\text{Si}(001)$ sys-

tem, where the phase sequence is inverted.^{17,18} We point out, however, that there are significant differences between these cases: continuous films are subject to lateral stress which is reduced or eliminated for islanded films; the continuous films are much thicker (~ 30 vs 2 nm) and they are prepared under non-UHV conditions, hence the interface quality is suspect. For these reasons, we believe that the relative stability of the hexagonal phase which we observe in these island structures is an intrinsic feature.

The central result of this paper is the observation that the NW islands grown at 650 °C have faulted surface layers. These layers are clearly associated with the NW itself, since they do not appear on the larger (wider and thicker) 3D islands. It is difficult to determine directly whether the faulted layers are a cause or an effect of the NW shape. However, since the tetragonal silicide has an isotropic lattice mismatch with $\text{Si}(001)$ of +5% each direction, it is not likely to be a *cause* for the highly anisotropic NW shape. We speculate that the NW begins growing coherently as hexagonal DySi_2 , with asymmetrical strain, but soon adopts faulted surface layers to provide stress relief for the underlying lattice. This hypothesis would explain why the faulted layers do not occur on the 3D islands, since the latter are strain free. The lack of strain is understandable, since the 3D islands are large and have highly stepped buried interfaces. Unfortunately, there are no calculations of critical (coherent) island size for DySi_2 on $\text{Si}(001)$ to guide this hypothesis. Steps at the buried interface are expected to reduce island stress as well, as they do in the well-documented $\text{Co}/\text{Si}(111)$ system.¹⁹

Careful inspection of Fig. 4 shows that the surface layers on the NW are incomplete and/or defective. We note that a vacancy row would comprise a structural basis for the trenchlike structures described as “nanowire bundles.”³ The presence of faulted surface layers and vacancy rows would provide a variable degree of stress relief in the NW. This may explain the lack of a well-defined width in this NW system.^{3,5}

This work was supported by NSF Grant Nos. DMR9981779 and ECS0304682(NIRT). We acknowledge use of facilities in the John M. Cowley Center for High Resolution Electron Microscopy.

¹C. Preinesberger, V. S. R. Kalka, and M. Dahne-Prietsch, *J. Phys. D* **31**, L43 (1998).

²C. Preinesberger, S. K. Becker, S. Vandre, T. Kalka, and M. Dahne, *J. Appl. Phys.* **91**, 1695 (2002).

³B. Z. Liu and J. Nogami, *J. Appl. Phys.* **93**, 593 (2003).

⁴J. Nogami, B. Z. Liu, M. V. Katkov, C. Ohbuchi, and N. O. Birge, *Phys. Rev. B* **63**, 233305 (2001).

⁵Y. Chen, D. A. A. Ohlberg, G. Medeiros-Riberiro, Y. A. Chang, and R. S. Williams, *Appl. Phys. Lett.* **76**, 4004 (2000).

⁶Y. Chen, D. A. A. Ohlberg, and R. S. Williams, *J. Appl. Phys.* **91**, 3213 (2002).

⁷K. L. Kavanagh, M. C. Reuter, and R. M. Tromp, *J. Cryst.*

Growth **173**, 393 (1997).

⁸M. Stevens, Z. He, D. J. Smith, and P. A. Bennett, *J. Appl. Phys.* **93**, 5670 (2003).

⁹Z. He, M. Stevens, D. J. Smith, and P. A. Bennett, *Surf. Sci.* **524**, 148 (2003).

¹⁰Z. He, M. Stevens, D. J. Smith, and P. A. Bennett, *Appl. Phys. Lett.* **83**, 5292 (2003).

¹¹J. L. McChesney, A. Kirakosian, R. Bennewitz *et al.*, *Nanotechnology* **13**, 545 (2002).

¹²P. A. Bennett and H. v. Kaenel, *J. Phys. D* **32**, R71 (1999).

¹³R. T. Tung, *Appl. Surf. Sci.* **117–118**, 268 (1997).

¹⁴R. T. Tung, *Mater. Chem. Phys.* **32**, 107 (1992).

- ¹⁵A. H. Reader, A. H. van Ommen, P. J. W. Weijs, R. A. M. Wolters, and D. J. Oostra, Rep. Prog. Phys. **56**, 1397 (1993).
- ¹⁶Z. Xu, *Properties of Metal Silicides* (INSPEC, London, 1995).
- ¹⁷A. Travlos, N. Salamouras, and E. Flouda, Appl. Surf. Sci. **120**, 355 (1997).
- ¹⁸A. Travlos, N. Salamouras, and N. Boukos, Thin Solid Films **397**, 138 (2001).
- ¹⁹H. von Kaenel, Mater. Sci. Rep. **8**, 193 (1992).